sustainability

MDPI

Article

A Novel Method for Estimating Biomass and Carbon Sequestration in Tropical Rainforest Areas Based on Remote Sensing Imagery: A Case Study in the Kon Ha Nung Plateau, Vietnam

Hoi Nguyen Dang [1], Duy Dinh Ba [1,*], Dung Ngo Trung [1] and Hieu Nguyen Huu Viet [2]

[1] Institute of Tropical Ecology, Joint Vietnam–Russia Tropical Science and Technology Research Center, № 63, Nguyen Van Huyen Str., Cau Giay District, Hanoi 122102, Vietnam
[2] Forest Inventory and Planning Institute (FIPI), Vinh Quynh Commune, Thanh Tri District, Hanoi 134500, Vietnam
* Correspondence: duydb.vrtc@gmail.com; Tel.: +84-989-331-023

Abstract: Forest ecosystems play a key role in sustaining life on this planet, given their functions in carbon storage, oxygen production, and the water cycle. To date, calculations of the biomass and carbon absorption capacity of forest ecosystems—especially tropical rainforests—have been quite limited, especially in Vietnam. By applying remote sensing materials, geographic information systems (GIS) facilitate the synchronized estimation of both biomass and ability of forest ecosystems to absorb carbon over large spatial ranges. In this study, we calculated the biomass of tropical rainforest vegetation in the Kon Ha Nung Plateau, Vietnam, according to four regression models based on Sentinel-2 satellite image data, forest reserve maps, and forest survey standard cell data (including 19 standard cells for 2016 and 44 standard cells for 2021). The results of the data comparison for the four biomass computing models (log-log, log-lin, lin-log, and lin-lin) demonstrated that the models with the highest accuracy were the lin-log model for 2016 (with a correlation coefficient of R^2 = 0.76) and the lin-log model for 2021 (with a correlation coefficient of R^2 = 0.765). Based on the analytical results and the selection of biomass estimation models, biomass maps were developed for the Kon Ha Nung Plateau area, Vietnam, in 2016 and 2021, with a predominant biomass value of 80–180 tons/ha (Mg/ha); furthermore, biomass fluctuations were analyzed for the period 2016–2021. Accordingly, the ability to absorb carbon and CO_2 equivalents in this research area for 2016 and 2021 was calculated based on the estimated biomass values. In summary, we present a method for estimating biomass via four basic linear regression models for tropical rainforest areas based on satellite image data. This method can serve as a basis for managers to calculate and synchronize the payment of carbon services, which contributes to promoting the livelihoods of local people.

Keywords: biomass; tropical rainforest; carbon; Sentinel-2; regression models

Citation: Dang, H.N.; Ba, D.D.; Trung, D.N.; Viet, H.N.H. A Novel Method for Estimating Biomass and Carbon Sequestration in Tropical Rainforest Areas Based on Remote Sensing Imagery: A Case Study in the Kon Ha Nung Plateau, Vietnam. *Sustainability* **2022**, *14*, 16857. https://doi.org/10.3390/su142416857

Academic Editor: Sharif Ahmed Mukul

Received: 11 September 2022
Accepted: 9 December 2022
Published: 15 December 2022

1. Introduction

Although tropical forests cover only approximately 10% of the world's total land area, they play a very important role in the global carbon and water cycle and are thought to be home to more than half of the world's species [1–3]. Evaluating and estimating the biomass and carbon absorption capacity of forest ecosystems is one of the basic research directions of forest scientists. Biomass generally consists of above and belowground organisms, such as the stems, branches, and leaves of trees, in addition to shrubs, vines, roots, fallen objects, and dead organic matters [4]. One method for biomass identification involves directly measuring predetermined standard cells in the field [5–12]. Due to the difficulties in collecting subterranean biomass data, relevant studies have mainly focused on terrestrial biomass estimates (AGB). In addition, many studies have shown that, with nests eventually comprising highly similar plants, biomass patterns may be established for most plant

species in some parts of the world; however, given the diversity of tropical forests, it is difficult to build and develop models for each specific species. In such cases, researchers often apply multispecies models with larger sample sizes, cutting down sample plants for measurement [5]. Chave et al. used 2410 sample trees to create common biomass models for tropical forests [13]. Later studies showed that the application of such a general biomass equation in the tropics can lead to systematic estimation errors of up to 400%; therefore, individual localized models may be a more suitable alternative, providing greater reliability than the general equation [14]. To improve the reliability of biomass models, Temesgen et al. proposed the development of a comprehensive biomass model including more relevant variables, such as density, height, and coverage, and following different spatial scales [15,16]. In addition, to improve model quality, studies have aimed at optimizing and reducing model errors or eliminating models with large deviations from reality (overfitting). In this line, the cross-validation method for biomass models has also been implemented by many authors around the world, including Zhang et al. (1997) [17]. In addition, cross-evaluation is also the basis for selecting appropriate variables for such a model [18].

To solve the problem that exists in the stated field investigation methods (i.e., standard celling and live metering), remote sensing techniques have been commonly applied for AGB estimation over the past two decades [19–22]. The ability to repeatedly photograph clear spaces, collect information, and monitor areas that have expanded has been demonstrated to contribute to the effectiveness of this method, which is becoming increasingly used for the estimation of cumulative growth and biomass yield across a range of forest areas [23]. In India, a method involving a high-precision land-use overlay map combined with remote sensing materials and GIS has been established and applied to identify excess biomass in wastelands in three states: Madhya Pradesh, Maharashtra, and Tamil Nadu [24]. In Poland's Upper Silesia and Kujawsko-Pomorskie provinces, remote sensing and GIS applications and secondary data sources were used to determine that the biomass of agricultural crops reached 0.60 tons/hectare (Mg/ha) over a 12-month period. These figures correspond to approximately 57,000 and 178,000 tons per year in these provinces [25]. In Vietnam, Landsat and Sentinel-2 images have also been used to calculate the biomass of mangroves in Quang Ninh Province and Thai Binh Province [26].

In the study of biomass and forest carbon, the use of appropriate algorithms for establishing biomass estimation models that combine information from remote sensing data is crucial. Regression analysis is the approach most frequently used for developing biomass estimation models. This approach often uses the results of biomass calculations in the sample cells as dependent variables, while the independent variables include spectral characteristics and plant indicators. These models assume that biomass variables are linearly correlated with spectral reactions [27]. Many regression correlation analyses have been used to predict forest biomass and have indicated that visual texture is an important variable for estimating biomass in adult forests [19,28,29]. Regression models can also be applied to enable AGB calculations in tropical rainforest areas. In Kalimantan, using an AGB-defined regression model for two hoard forests and peat bogs resulted in an accuracy rate of 71% with RMSE = 33.85% [30]; this model has also been applied in Norway [31] and Ontario [32]. The use of plant indices to determine forest biomass has also been extensively reported in previous studies. At the National Nature Reserve of Yaoluoping in Anhui Province, China, the NDVI_DR index was applied to estimate biomass with results of R^2 = 0.63 and RMSE = 11.18 Mg/ha for broadleaf forests and R^2 = 0.61 and RMSE = 14.26 Mg/ha for coniferous forests [33].

For tropical rainforests, the identification of AGB based on remote sensing imagery still has many limitations and faces certain difficulties. Using optical remote sensing imaging to calculate AGB can be affected by various factors, such as the complexity of the forest structure or environment, in addition to canopy and topographic shadow that adversely impact the calculation results for biomass on the forest ground [7,34]. In wet tropical forests, studies have estimated that AGB is constrained by complex stand structures, high species composition diversity, and divergences between different periods of forest ecosystem

development [22,35]. AGB is determined by the distribution of species, tree size and height, and the structure of each type of forest [36]. In addition, the tropical rainforest structure is also quite complex and heterogeneous, with dense canopies [37]. The structure and AGB of tropical rainforests can be influenced by a variety of factors, such as climate [38] and human activities [39,40]. Remote sensing imagery is also affected by cloud cover in tropical areas, leading to difficulties in analyzing and processing data [41].

The application of remote sensing technology combined with survey data, field surveys, and actual biomass calculations based on the establishment of standard cells allows for the determination of AGB with high accuracy while saving time and cost, compared to conventional field survey methods. Vietnam is a country in the tropical monsoon region, with a diverse and rich tropical rainforest ecosystem including many different types of forests. However, with three-quarters of the natural area being hilly, including many hard-to-reach areas, the application of remote sensing and GIS technology combined with survey data, field surveys, and biomass estimates allows for the determination of forest ecosystem biomass on a large and synchronous scale. The area of the Kon Ha Nung Plateau in Gia Lai Province, Vietnam, includes Kon Ka Kinh National Park and Kon Chu Rang Nature Reserve, which feature high biodiversity and a forest ecosystem characteristic of the Central Highlands provinces, with many unique and outstanding features and characteristics [42]. Currently, the policies of the Kon Ha Nung Plateau region, as well as those in Vietnam in relation to forest environmental service payment, especially policies related to carbon services, have not been implemented. The method of estimating biomass and calculating the carbon coefficient still has many shortcomings and is not synchronous. This causes many difficulties with regard to paying for forest environmental services, affecting the rights of local people. Therefore, it is necessary for managers to build a model that estimates biomass, as well as carbon sequestration capacity, to develop relevant policies.

In this study, we used Sentinel-2 satellite imagery from 2016 and 2021 combined with standard forest survey cell measurement data to estimate the biomass of tropical rainforest vegetation in the Kon Ha Nung Plateau area, Vietnam. Four basic regression models were applied to forest vegetation biomass estimates based on NDVI values for satellite imagery, forest reserve data, and forest survey standard cell data. From there, we compared the accuracy of the model through the R^2 coefficient and selected the most accurate model for the study area. The main objectives of this study include (1) selecting an appropriate biomass estimation model for the rainforest ecosystem in the Kon Ha Nung Plateau area and (2) developing biomass, carbon stock, and CO_2 equivalent values for the period 2016–2021 for forest vegetation in the Kon Ha Nung Plateau area, Vietnam. The obtained results may serve as a basis for planning policies to protect and develop forest ecosystems through biodiversity conservation and reasonable use of the territory.

2. Materials and Methods

2.1. Study Area

The Kon Ha Nung Plateau area is a mountainous area east of the Truong Son Range, located in northeastern Gia Lai Province, approximately 100 km from Pleiku City along National Highway 19 and Truong Son Dong National Highway, with a total natural area of 2429.33 km^2 (Figure 1). The region is bordered as follows:

+ To the north by Kon Plong district (Kon Tum province);
+ To the east by Quang Ngai and Binh Dinh provinces;
+ To the south by An Khe town and Dak Po district, Gia Lai province;
+ To the west by Chu Păh district, Gia Lai province.

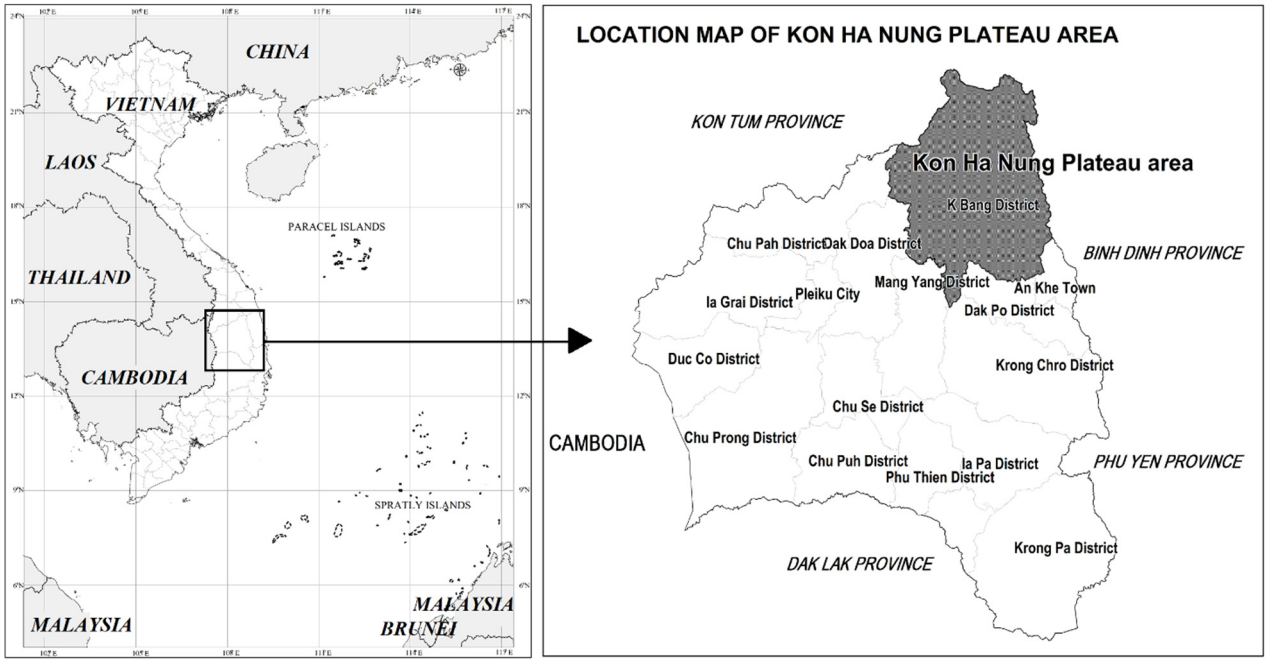

Figure 1. Location of the Kon Ha Nung Plateau area.

The Kon Ha Nung Plateau has a fairly diverse geological composition, in which basalt typically forms the ancient plateau of Kon Ha Nung, stretching from the southeast of Kon Plong district (Kon Tum) to the south of K'Bang district and bordering the An Khe lowland, along with a medium and a low mountain system on granite. The terrain of the divided area is quite complex, including mountainous terrains, hills, valleys, and plateaus. In particular, the average mountainous terrain is mainly distributed in the western area of Kon Ka Kinh National Park. The level of separation is strong, the slope is typically high, and the elevation ranges up to 1748 m above sea level [43]. To the east of the study area are mainly vast basalt plateaus, the terrain of which is relatively flat. Climatically, the study area belongs to the tropical monsoon highland climate zone. The average temperature is 23.5 °C, the dry season lasts from January to April, the rainy season lasts from May to December every year, and there is a high average annual rainfall ranging from 1500–2800 mm [44]. Forests and forest resources are the richest land type in the Central Highlands and the whole country, with the area of primeval forests concentrated in two special-use forests: Kon Ka Kinh National Park and Kon Chu Rang National Park. In addition to the oily plants forming low-lying ecosystems at <1000 m elevation, coniferous species, such as *Pinus dalatensis* and *Dacrydium elatum*, have been recorded in the area, along with many trees of high economic value, such as *Pterocarpus macrocarpus*, *Citrus sinensis*, and *Dysoxylum loureirii*. The fauna is also rich and diverse, with 49 animal, 221 bird, 50 reptile, and 25 frog species, many of which are of conservation value and can be found on the IUCN Red List [45].

2.2. Materials

2.2.1. Satellite Image Data

In the Kon Ha Nung Plateau area, January–March is the end of the dry season, with very little rain. As such, satellite imagery of the study site during this period is virtually unaffected by cloud factors as well as other atmospheric factors, consistent with the quality and timing of image acquisition. Based on the temporal selection corresponding to when satellite imagery had the lowest cloud cover during this period, we used Sentinel-2 satellite imagery data from 2016 and 2021 to map land-use coverage in the Kon Ha Nung Plateau, Gia Lai Province, Vietnam (Table 1). Sentinel-2 satellite imagery in the selected periods was not affected by clouds, ensuring accuracy during image processing.

Table 1. Technical parameters and acquisition time of Sentinel-2 remote sensing images.

Date	Sensor	Image Bands	Resolution
13/02/2016	Sentinel-2	Blue (0.455–0.525 μm), Green (0.530–0.590 μm), Red (0.625–0.695 μm), Near-Infrared (0.760–0.890 μm)	Panchromatic: 10 m × 10 m Multispectral: 20 m × 20 m
16/02/2021	Sentinel-2	Blue (0.455–0.525 μm), Green (0.530–0.590 μm), Red (0.625–0.695 μm), Near-Infrared (0.760–0.890 μm)	Panchromatic: 10 m × 10 m Multispectral: 20 m × 20 m

2.2.2. Standard Cells for Forest Investigation

For data of standard cells for forest investigation, the standard cell ground investigation results were used, according to the design of the standard cluster of forest survey standards of the project of surveying, evaluating, and monitoring national forest resources in the period 2016–2020 presided over by the Ministry of Agriculture and Rural Development of Vietnam (including 19 cells of natural forest investigation standards in the research area). In 2021, standard forest investigation cells were investigated in Gia Lai Province (a total of 44 boxes of forest investigation standards). All field surveys and data collection for forest standard plots were conducted at the end of the dry season (February and March) in 2016 and 2021, consistent with the Sentinel-2 image selection timeline. Forest standard cell measurement techniques were implemented based on the circulars and guidelines of the Ministry of Agriculture and Rural Development of Vietnam (Circular No. 25/2009/TT-BNN and Decision No. 689/QD-TCLN-KL for 2016; Circular No. 33/2018/TT-BNNPTNT for 2021). This served as the basis for calculating, identifying real biomass, and comparing and evaluating the accuracy with biomass calculation models based on remote sensing imagery through the various stages.

Standard groups of cells were based on grid cells with a distance of 8 km × 8 km. In each group of cells, 5 circle-shaped cells were set up in the form of an L-shape, and the sample cell area was 400 m^2/cell (20 m × 20 m). The distance between the center of 2 adjacent sample cells was 150 m. The center of denominator cell No. 3 coincided with the center of the cell group. The standard cell had the form of a square, and the length of the cell side was 20 m (Figure 2). The trees in the standard cell were defined species names, which were used for measuring the diameter and height of the trees to determine the biomass of the standard cell.

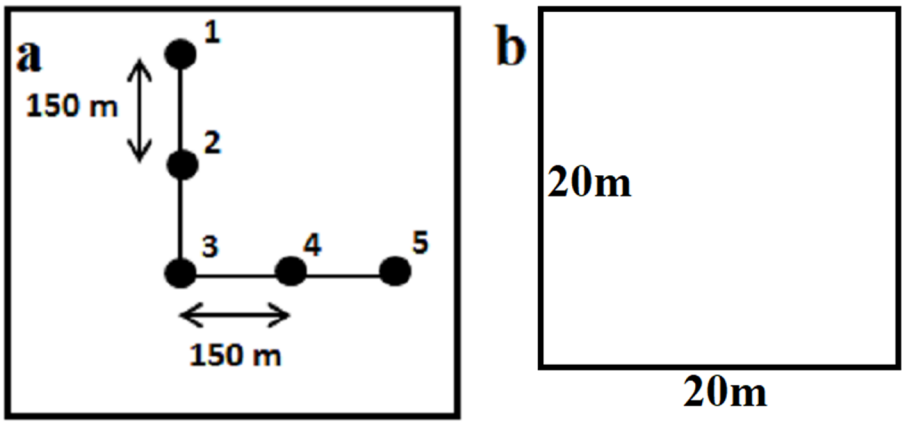

Figure 2. Standard cell group shape of 5 cells (**a**) and size per standard cell (**b**).

The formula for calculating biomass based on standard cell data was proposed by Chave (2014) [14] as follows:

$$AGB_{est} = 0.0673 \times \left(\rho D^2 H\right)^{0.976} \quad (1)$$

2.3. Methods

2.3.1. Research Process

The framework for processing remote sensing imagery combined with field survey data from the forest investigation standard cells is presented in Figure 3. In particular, for Sentinel-2 data in 2016 and 2021, the spectral radiation correction was performed according to the formula:

$$\rho_{BOA,\,\lambda} = \frac{\pi \times L_\lambda}{A_{k,NTDI} \times E_s \times d(t) \times \cos(\theta_s(i,j))} \quad (2)$$

where

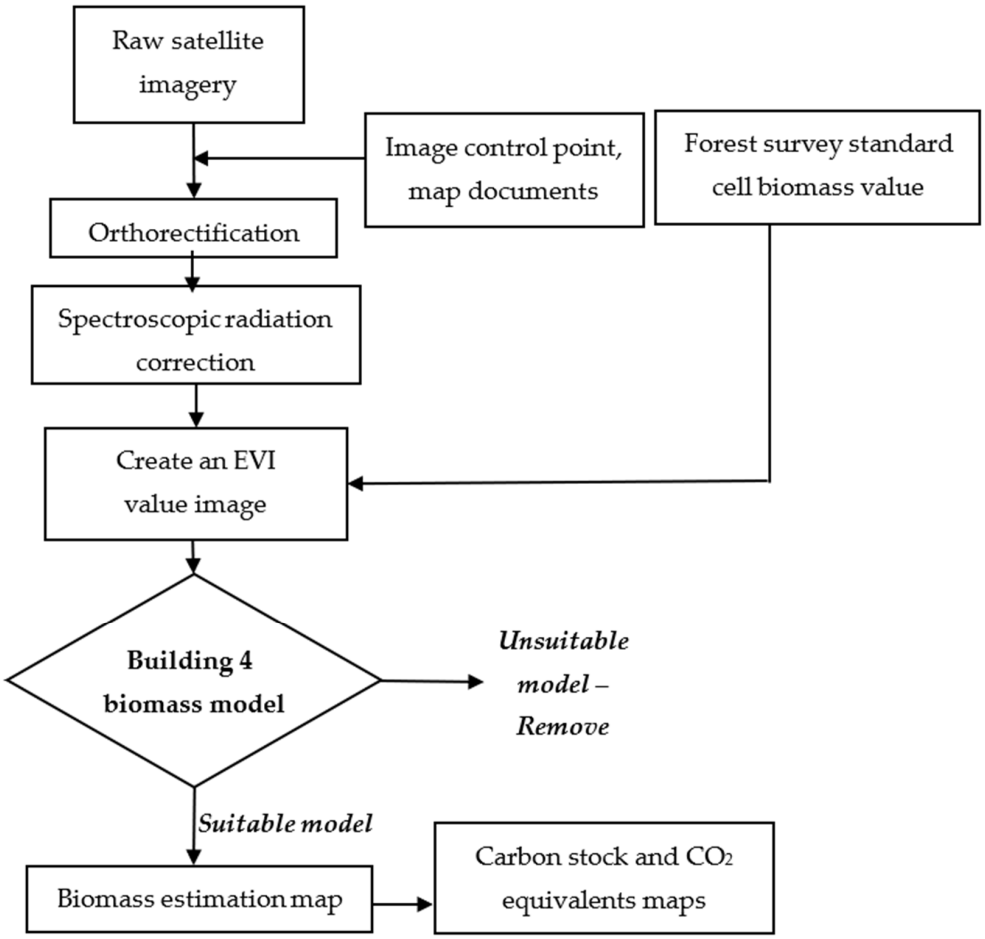

Figure 3. The process of creating biomass value maps from remote sensing imagery.

$A_{k,NTDI}$ is the absolute calibration value of the device (provided by GIPP and taken in the metadata file of the image);

E_s is the average solar spectral radiation value (provided by GIPP and taken in the metadata file of the image);

θ_s is the peak angle (included in the Sentinel image metadata file);

$d(t)$ is the astronomical distance between the Earth and the Sun, determined according to the formula:

$$d(t) = \frac{1}{(1 - 0.01673 \times \cos(0.0172 \times (t-2)))^2} \quad (3)$$

2.3.2. Selecting the Formula and Specifying Parameters for the Model

Weighting for Forest Types

The map of forest reserves was based on the results of Sentinel-2 image analysis in 2016 and 2021 from our project, which is chaired by the Joint Vietnam–Russia Tropical Science and Technology Research Center from 2022 to 2023. Accordingly, forest types and forest reserves were identified based on circular 34/2009/TT-BNNPTNT on forest criteria and classification regulations of the Government of Vietnam to determine the weight for each forest type, according to Table 2:

Table 2. Forest encoding types in the study area.

№	ldlr	Forest Type	Reserves	Weighting
1	RLP	Natural wood forests of mountainous land with evergreen broadleaf forest restored	Forest restoration	1
2	TXP	Evergreen broadleaf forest restored	Forest restoration	1
3	TNK	Natural bamboo forests of soil mountains	Very poor forests	2
4	TXK	Poor evergreen broadleaf natural timber forests	Very poor forests	2
5	TXN	Natural timber forests of mountainous land with poor evergreen broadleaf lands	Poor forests	3
6	RKB	Mountain coniferous forest with medium reserves	Medium forest	4
7	TXB	Natural timber forests on mountainous land with medium evergreen broadleaves	Medium forest	4
8	TXG	Natural timber forest in mountains with rich evergreen broadleaf land	Rich forest	5

Agricultural soils, plantations, and other land types (e.g., rural land, water surfaces) are not natural forest ecosystems and, thus, were not evaluated for biomass in this study.

Determination of the EVI Based on Remote Sensing Data

Enhanced vegetation index (EVI) was invented by Liu and Huete to simultaneously calibrate the value of NDVI against atmospheric influence and ground reflections, especially in areas with dense canopies. The value range of EVI is −1 to 1, and for healthy vegetation, the value ranges between 0.2 and 0.8. According to Xue et al., EVI can improve the vegetation signal by decoupling the canopy background signal and reducing the atmospheric signal in high biomass regions, as well as improving vegetation monitoring. Besides, EVI is more responsive to type, canopy variations, and architecture and can be responsive to vegetation stress [46]. The formula for calculating the EVI is as follows [47]:

$$EVI = 2.5\frac{R_{nir} - R_r}{R_{nir} + 6R_r - 7.5R_b + 1} \quad (4)$$

where the spectral values of the wave channels are as follows: blue (R_b) 450 nm ± 16 nm; red (R_r) 650 nm ± 16 nm; and near-infrared (R_{nir}) 840 nm ± 26 nm.

Defining the Biomass Regression Models

To compare the accuracy of regression models for estimating forest biomass values, four common formulas were considered [48]:

1. Log-Log Paradigm:

$$\log_{10}(\text{AGB}) = \text{a} \times \log_{10}(\text{EVI value}) + \text{b} \times \text{ldlr} + \text{c} \quad (5)$$

2. Log-Lin Paradigm:

$$\log_{10}(\text{AGB}) = \text{a} \times (\text{EVI value}) + \text{b} \times \text{ldlr} + \text{c} \quad (6)$$

3. Lin-Log Paradigm:

$$AGB = a \times \log_{10}(EVI\ value) + b \times ldlr - c \quad (7)$$

4. Lin-Lin Paradigm:

$$AGB = a \times (EVI\ value) + b \times ldlr - c \quad (8)$$

Selection of the appropriate model involved the selection of a function with weights that reflect the strong, objective interaction between the biomass value variable and the remote sensing spectroscopic reflection. An effective tool for tackling the abovementioned technology is based on regression function theory with high-level processing and image combinations. This step involved examining and evaluating measurements estimated with respect to the biomass value image and then verifying the result using the standard monitoring data from the forest investigation conducted at the same time that the data were collected.

The 4 selection models represent 4 common forms of linear regression models. Sometimes, experimentally, if we take the original value, the difference between the largest value and the smallest value is extremely large. When the log is removed, the deviation in the data decreases, which is more in line with the model assumption (the model usually assumes the data have a standard distribution, and the deviation must also be within a certain limit from the mean). Through the experimental process, depending on the time of image acquisition and the characteristics of the study area, the best model is selected. In this study, the right model was selected by comparing the Pearson correlation coefficients of the models with one another and taking the model with the highest value.

Verification of the Model Accuracy

Based on a map of the current state of vegetation established from remote sensing imagery, along with the biomass data of 19 standard cells for forest investigation in 2016 and 44 cells of forest investigation standards in 2021, we examined the accuracy of the model (Figure 4).

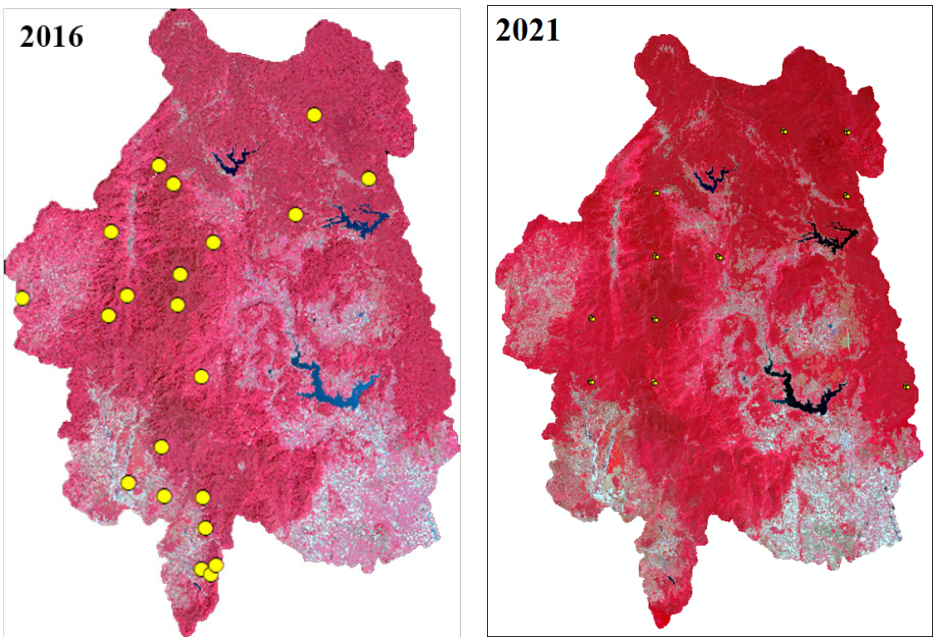

Figure 4. Pseudo-colored (Nir-Red-Green) composite photos of Sentinel-2 photos in 2016 and 2021, with standard forest investigation cells labeled in yellow.

The mapping of biomass reserves begins by establishing the correlation between variables, including vegetation status maps, forest reserve classification maps, remote sensing EVI values, and biomass data calculated based on the standard forest survey of 19 cells in 2016 and 44 cells in 2021, through correlation analysis and linear regression. Before conducting these analyses, the standard Kolmogorov-Smirnov test was applied to both sources of data to assess whether they met the standardization requirements for the data in the statistical model. Excel was used to analyze the relationship between the EVI values in the images. The status quo categorized the classified forest reserves and the actual AGB values according to the forest investigation standard cell, and we calculated a coefficient (r) to indicate their correlation level. In particular, the EVI and the status quo that classified forest reserves were taken as the independent variables, and the AGB was the dependent variable. With these, the following initial linear equation was identified: $y = a \cdot x + b$.

The Pearson correlation coefficient for two variables x and y from n samples was calculated according to the formula:

$$R^2 = \frac{\sum_{i=1}^{n}\left[\left(Y_i - \overline{Y}_i\right)\left(X_i - \overline{X}_i\right)\right]}{\sqrt{\sum_{i=1}^{n}\left(Y_i - \overline{Y}_i\right)^2 \times \sqrt{\sum_{i=1}^{n}\left(X_i - \overline{X}_i\right)^2}}} \quad (9)$$

where Y_i and $\overline{Y}_i$ are the estimated variables and their averages, respectively;

X_i and $\overline{X}_i$ are the measurement variables and their average values, respectively;

n is the number of samples in the data set.

If $R^2 = 1$, the relationship between x and y can be determined; that is, for any value of x, we can determine the value of y. If $R^2 = 0$, the two variables x and y are completely independent, and they have no relation to each other. The R value is classified as follows: $0.3 \leq R^2 < 0.5$ indicates low correlation, $0.5 \leq R^2 < 0.7$ indicates moderate correlation, and $0.7 \leq R^2$ indicates high correlation [49].

We used standard errors (SEs) to assess the quality and quantity of biomass reserves (i.e., the AGB obtained from the linear regression analysis) in comparison to the biomass reserves measured in the field. The lower the SE value is, the higher the accuracy.

2.3.3. Method of Determining Carbon Reserves

From the survey data in the standard cell system, biomass models were used to estimate biomass, thereby calculating the equivalent carbon and CO_2 for each sample cell and, then, for the overall forest. In this study, carbon and CO_2 reserves equivalent to forest trees were calculated using the following conversion formulas:

$$\text{Carbon stock} = 0.47 \times \text{Biomass} \quad (10)$$

$$CO_2 \text{ equivalents} = 3.67 \times \text{Carbon stock} \quad (11)$$

3. Results

3.1. Determination of the EVI Based on Sentinel-2 Satellite Images

Based on Formula 3, EVI maps were built based on the Sentinel-2 satellite imagery from 2016 and 2021 (Figure 5).

Accordingly, the EVI value in the Kon Ha Nung Plateau area ranged from −0.24 to 0.98 in 2016 and from −0.29 to 0.96 in 2021. The areas with high EVI values (>0.4) were concentrated in the north and northeast (Kon Chu Rang Nature Reserve area), east (Kon Ha Nung Plateau watershed protection forest area), and west (Kon Ka Kinh National Park area). These are areas with high natural forest coverage, which are strictly protected.

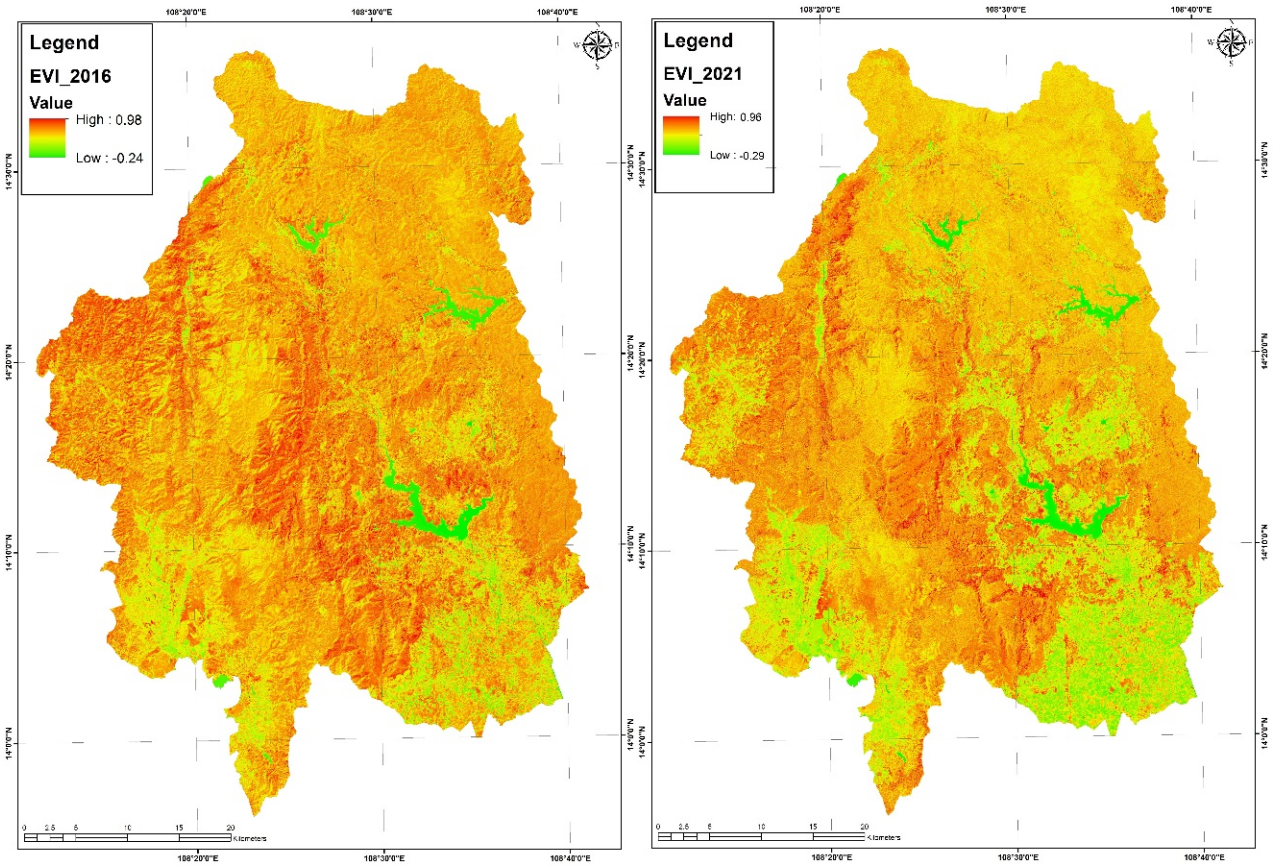

Figure 5. EVI based on remote sensing data for the Kon Ha Nung Plateau area in 2016 and 2021.

3.2. Defining the Biomass Estimation Model

3.2.1. Biomass Estimation Model for 2016

Based on Formula (4), regression models for the estimation of forest biomass values and correlation assessments were developed for the 2016 data, as detailed in Table 3 and Figure 6.

Table 3. Results of the regression models for 2016.

Name	Paradigm	R^2	RMSE
Log-Log Paradigm	$\log_{10}(AGB) = -1.5 \times \log_{10}(EVI\ 2016) + 0.12 \times ldlr + 2.00$	0.62	0.021
Log-Lin Paradigm	$\log_{10}(AGB) = -1.19 \times EVI\ 2016 + 0.12 \times ldlr - 3.08$	0.60	0.020
Lin-Log Paradigm	$AGB = -1370.8 \times \log_{10}(EVI\ 2016) + 217.11 \times ldlr - 223.22$	0.76	21.24
Lin-Lin Paradigm	$AGB = -1028.7 \times EVI\ 2016 + 218.57 \times ldlr - 706.03$	0.74	20.89

As such, for 2016, the lin-log model was chosen as the best-performing regression model. To evaluate the abovementioned construction model, we determined the root mean square error (RMSE) and the mean absolute error (MAE), as well as the correlation coefficient between the field data and the extracted data from the model and the modeling efficiency (ME) index. The results of the evaluation are shown in Table 4.

3.2.2. Biomass Estimation Model for 2021

Based on Formula (4), regression models for the estimation of forest biomass values and correlation assessments were also developed for the 2021 data, as detailed in Table 5 and Figure 7.

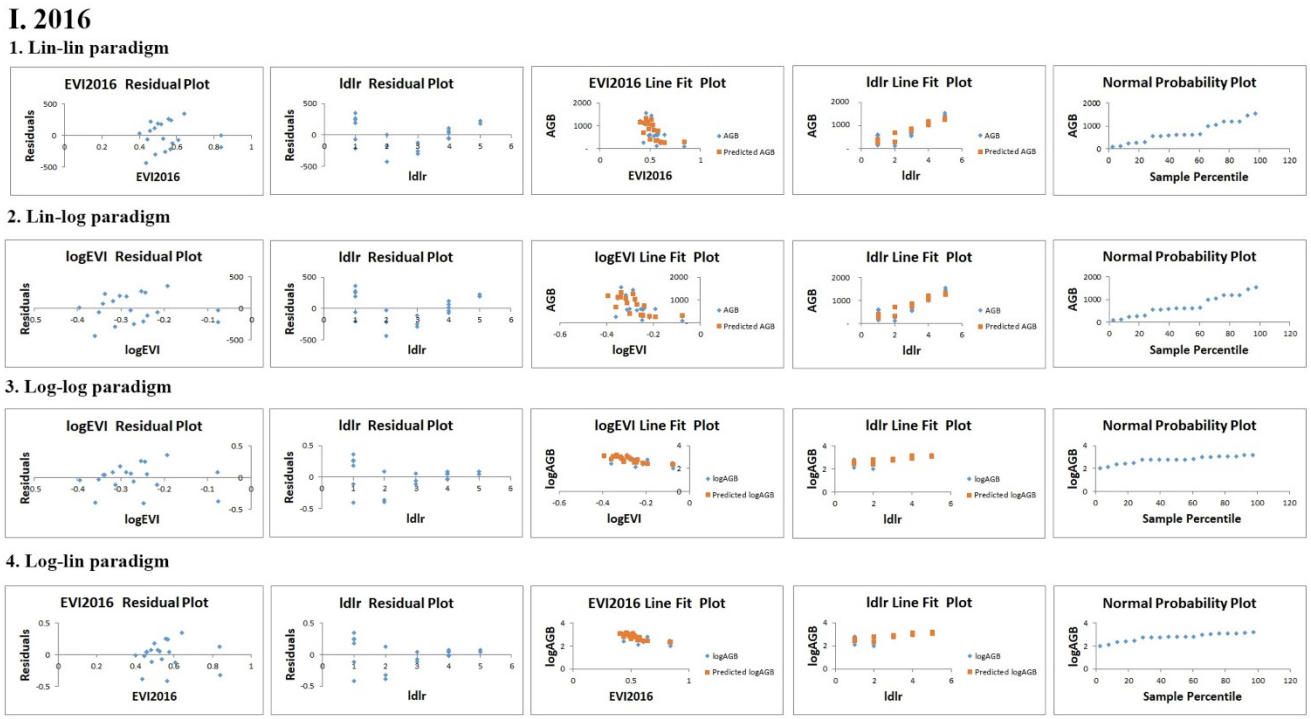

Figure 6. Assessment of four models for estimating the biomass of forest ecosystems in the Kon Ha Nung Plateau area in 2016.

Table 4. Biomass regression model construction accuracy for 2016 (unit: Mg/ha).

Forest Survey Cell Number	Field Data ($M_{TĐ}$)	Component Model (M_{AH})	dM = $M_{TĐ}$ − M_{AH}	Forest Survey Cell Number	Field Data ($M_{TĐ}$)	Component Model (M_{AH})	dM = $M_{TĐ}$ − M_{AH}
1	99.242	103.742	−4.500	11	118.252	111.099	7.153
2	106.111	112.233	−6.122	12	144.594	126.758	17.837
3	22.869	29.946	−7.077	13	155.022	132.560	22.462
4	12.916	34.313	−21.397	14	26.351	69.342	−42.991
5	55.255	80.952	−25.698	15	56.592	86.118	−29.526
6	61.296	35.082	26.214	16	64.668	76.934	−12.266
7	28.668	28.170	0.498	17	58.067	33.822	24.245
8	10.128	27.996	−17.867	18	60.495	41.161	19.334
9	119.860	108.558	11.302	19	61.378	26.528	34.850
10	120.180	116.632	3.547				
Total	72.734	72.734					
RMSE			20.892				
MAE			17.625				
R^2			0.76				

Table 5. Results of the construction of regression models for 2021.

Name	Paradigm	R^2	RMSE
Log-Log Paradigm	$\log_{10}(AGB) = 0.29 \times \log_{10}(EVI\ 2021) + 0.23 \times ldlr + 2.16$	0.758	0.08
Log-Lin Paradigm	$\log_{10}(AGB) = 0.28 \times EVI\ 2021 + 0.23 \times ldlr + 1.93$	0.761	0.07
Lin-Log Paradigm	$AGB = 701.8 \times \log_{10}(EVI\ 2021) + 508.9 \times ldlr - 807.2$	0.765	16.12
Lin-Lin Paradigm	$AGB = 646.0 \times EVI\ 2021 + 508.2 \times ldlr - 1342.01$	0.762	16.10

Thus, the best-performing regression model was the lin-lin model. The corresponding RMSE and MAE values are provided in Table 6.

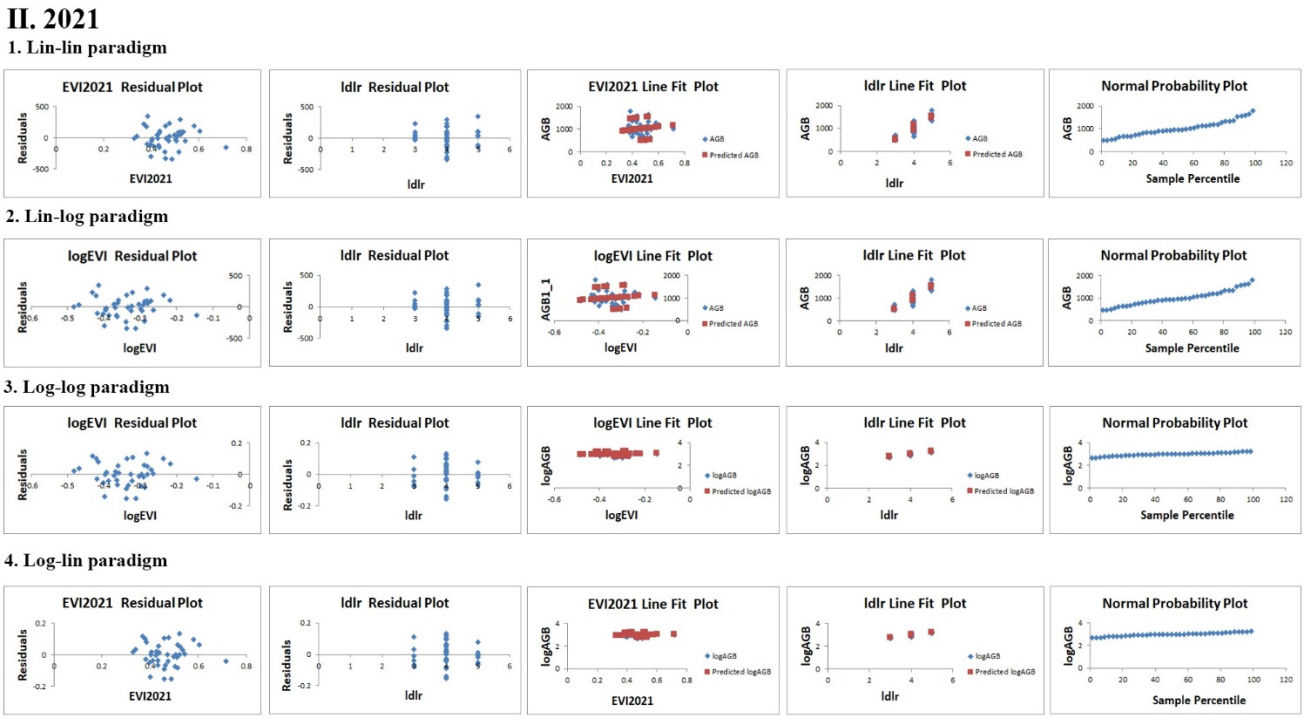

Figure 7. Evaluation of four models for estimating the biomass of forest ecosystems in the Kon Ha Nung Plateau area in 2021.

Table 6. Biomass regression model construction accuracy for 2021 (unit: Mg/ha).

Forest Survey Cell Number	Field Data ($M_{TĐ}$)	Component Model (M_{AH})	dM = $M_{TĐ}$ − M_{AH}	Forest Survey Cell Number	Field Data ($M_{TĐ}$)	Component Model (M_{AH})	dM = $M_{TĐ}$ − M_{AH}
1	151.666	147.584	4.082	23	62.379	52.927	9.452
2	179.189	144.597	34.592	24	93.431	89.943	3.488
3	82.716	95.643	−12.928	25	95.811	96.944	−1.132
4	93.431	95.241	−1.810	26	118.235	99.142	19.093
5	115.634	92.497	23.136	27	118.548	107.476	11.073
6	84.423	97.163	−12.740	28	125.530	106.208	19.322
7	65.031	94.883	−29.851	29	89.629	88.954	0.675
8	104.404	97.402	7.002	30	75.692	99.039	−23.347
9	80.023	102.603	−22.580	31	65.531	99.093	−33.562
10	66.722	100.859	−34.137	32	108.740	103.170	5.570
11	83.449	93.452	−10.003	33	132.236	103.040	29.196
12	132.919	148.186	−15.267	34	111.167	102.523	8.645
13	134.061	145.508	−11.447	35	72.245	49.341	22.904
14	163.309	153.968	9.341	36	96.484	102.033	−5.549
15	94.475	99.950	−5.475	37	99.385	104.256	−4.871
16	47.608	48.492	−0.884	38	99.862	112.605	−12.742
17	51.052	49.289	1.762	39	156.238	153.256	2.983
18	90.370	95.047	−4.676	40	62.379	52.927	9.452
19	111.737	93.294	18.443	41	93.431	89.943	3.488
20	159.021	148.423	10.597	42	95.811	96.944	−1.132
21	55.366	50.644	4.721	43	118.235	99.142	19.093
22	47.919	50.994	−3.075	44	118.548	107.476	11.073
Total	*100.402*	*100.402*					
RMSE			16.118				
MAE			12.612				
R^2			0.765				

According to the data from Table 6, the following can be noted:

The correlation coefficient between the construction model and the field sample component data was 0.873.

According to the field data from the sample analysis, the biomass ranged from 47.608 to 179.189 Mg/ha.

In terms of real errors, the RMSE and MAE had values of ±16.118 and 12.612, respectively.

3.3. Mapping the Estimated Biomass Value and Natural Forest Carbon Reserves in the Kon Ha Nung Plateau Area

Based on the high-precision regression models (lin-log model for 2016 and log-lin model for 2021), biomass estimates were established for the Kon Ha Nung Plateau area in 2016 and 2021 (Figure 8).

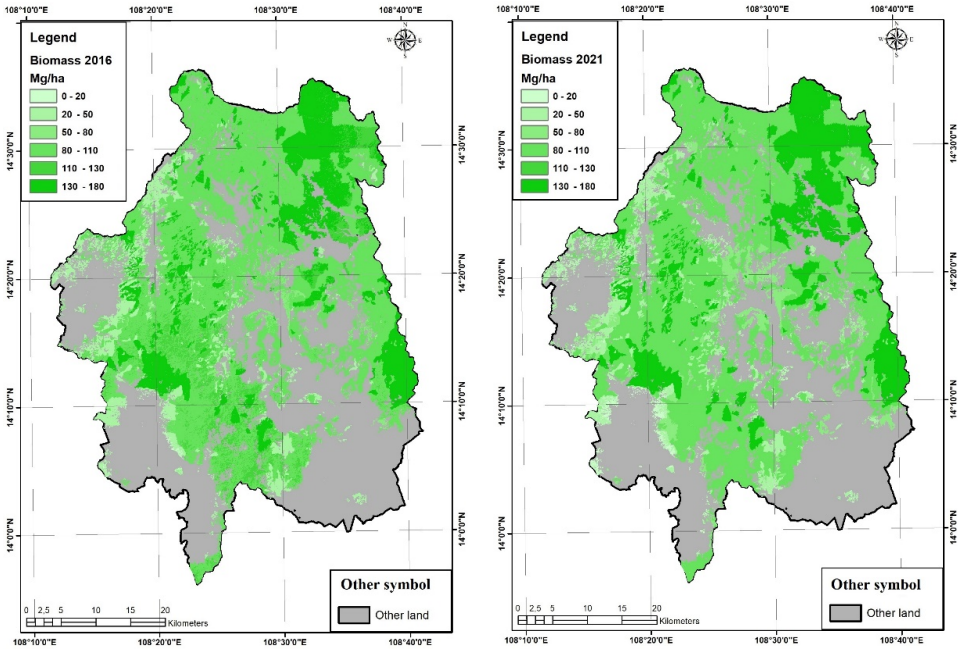

Figure 8. Biomass values in the Kon Ha Nung Plateau area in 2016 and 2021.

Accordingly, in 2016, the areas with biomass values in the range of 800–110 Mg/ha had an area of over 86,000 ha, accounting for 58% of the total area of natural forests. Meanwhile, the areas with biomass values in the range of 0–20 Mg/ha had the smallest total area, with slightly more than 1000 hectares (accounting for 0.69% of the total natural forest area). For the biomass value range of 130–180 tons per hectare, the area ratios in 2016 and 2021 were 20.09% and 22.45%, respectively. The biomass value range of 110–130 Mg/ha showed marked fluctuations in 2016 and 2021, decreasing from nearly 14,000 hectares in 2016 to approximately 80 hectares in 2021 (Table 7).

Table 7. Natural forest biomass results for the Kon Ha Nung Plateau area in 2016 and 2021 (biomass units: Mg/ha).

Biomass Value (Mg/ha)		0–20	20–50	50–80	80–110	110–130	130–180
2016	area (ha)	1030.28	14,768.66	3038.61	86,377.44	13,941.46	30,126.35
	%	**0.69**	**9.85**	**2.03**	**58.05**	**9.30**	**20.09**
2021	area (ha)	2375.05	13,732.54	10,190.75	89,242.08	78.85	33,663.53
	%	**1.58**	**9.16**	**6.80**	**59.51**	**0.51**	**22.45**

The areas with high biomass values were concentrated in the core area of Kon Chu Rang Nature Reserve, Kon Ka Kinh National Park, and the watershed protected forest

area southeast of Kon Ha Nung Plateau. These are areas with dominant evergreen forest ecosystems, with structures that are stable and strictly protected. Meanwhile, the areas with low biomass values were concentrated in the southern Kon Ha Nung Plateau and the western area of Kon Ka Kinh National Park (Figure 8).

Based on the results of biomass estimates for 2016 and 2021 and Formulas (10) and (11), carbon stocks and CO_2 equivalents in the Kon Ha Nung Plateau region were mapped for 2016 and 2021 (Figure 9 and Table 8)

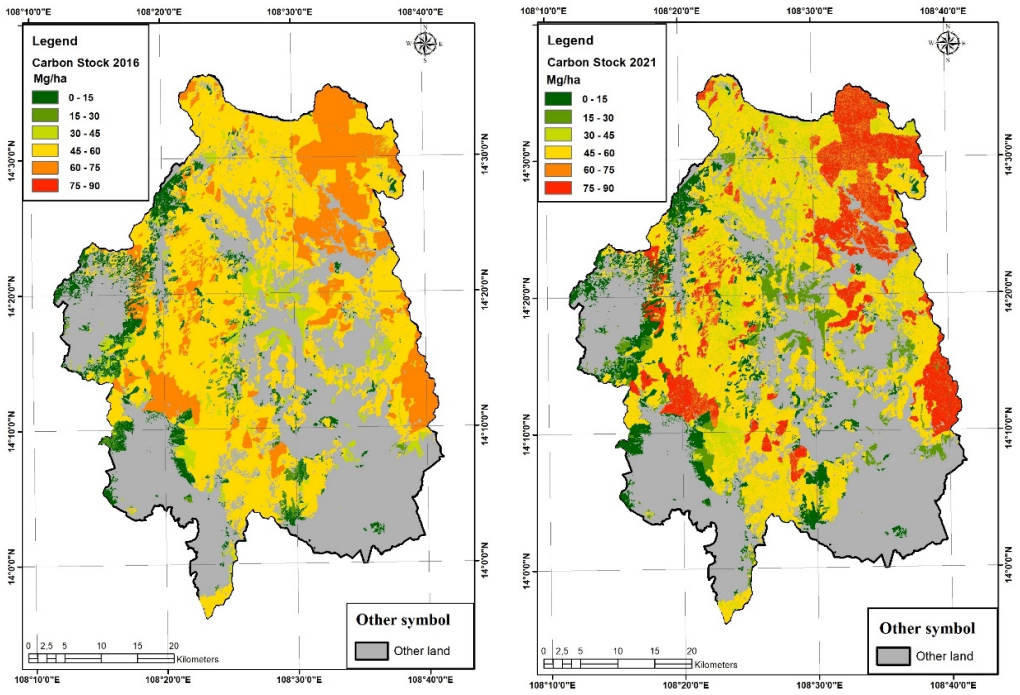

Figure 9. Carbon stocks in the Kon Ha Nung Plateau area in 2016 and 2021.

Table 8. Carbon stock value and CO_2 equivalents in the natural forests on the Kon Ha Nung Plateau in 2016 and 2021.

Carbon Stock Value (Mg/ha)		**0–15**	**15–30**	**30–45**	**45–60**	**60–75**	**75–90**
2016	area (ha)	12,333.5	3939.65	9737.48	90,082.55	33,189.62	0
	%	**8.22**	**2.63**	**6.49**	**60.52**	**22.13**	**0.00**
2021	area (ha)	15,002.6	10,324.22	20,991.8	69,288.01	9943.58	23,732.57
	%	**10.00**	**6.88**	**14.00**	**46.20**	**7.09**	**15.83**
CO_2 equivalents value (Mg/ha)		**0–60**	**60–120**	**120–180**	**180–240**	**240–300**	**300–320**
2016	area (ha)	15,729.6	593.73	16,277.84	116,681.66	0	0
	%	**10.49**	**0.40**	**10.85**	**78.26**	**0.00**	**0.00**
2021	area (ha)	15,099.1	10,492.11	89,589.17	510.25	33,574.43	17.77
	%	**10.07**	**7.00**	**59.74**	**0.34**	**22.84**	**0.01**

According to the data in Table 8, the areas with carbon stock values between 45 and 60 tons per hectare had an area of over 90,000 hectares, accounting for over 60% in 2016 and over 46% in 2021 (Table 8). Natural forest areas with carbon stock values in the range of 75–90 Mg/ha in 2021 increased sharply, from 0% to 15.83% of the total natural forest area in the Kon Ha Nung Plateau area, and were distributed mainly in the core area of Kon Chu Rang Nature Reserve (Figure 9). Meanwhile, the areas of natural forest with low carbon stock values were concentrated mainly west of Kon Ka Kinh National Park and south of Kon Ha Nung Plateau.

In 2016, the areas with CO_2 equivalent values between 180 and 240 tons per hectare had an area of 116,000 hectares, accounting for 78.26% of the total natural forest area, while in 2021, the areas with CO_2 equivalent values between 120 and 180 Mg/ha accounted for the largest area, accounting for nearly 60% of the total natural forest area. The areas with CO_2 equivalents reaching a value of 240–320 Mg/ha presented a strong increase in area in the period 2016–2021, with a total area of over 33,500 hectares, and were concentrated in the core area of Kon Chu Rang Nature Reserve, southwest of Kon Ka Kinh National Park, and the watershed protected forest area southeast of the Kon Ha Nung plateau (Figure 10).

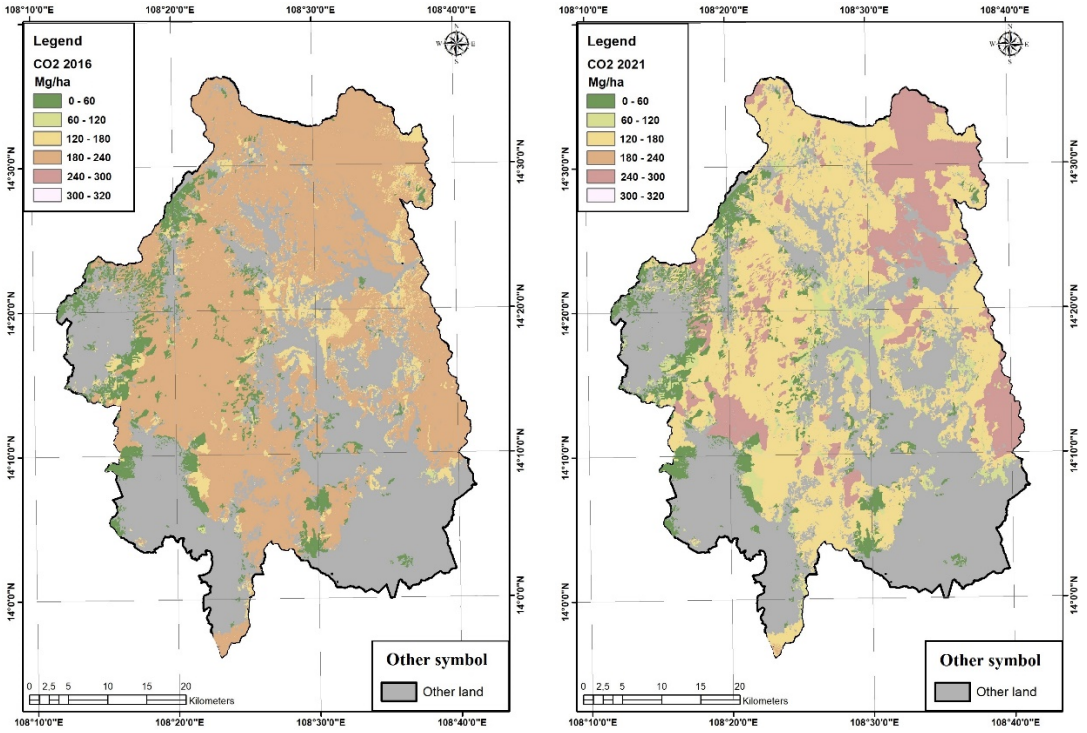

Figure 10. CO_2 equivalents in the Kon Ha Nung Plateau area in 2016 and 2021.

4. Discussion

4.1. Estimation of Tropical Rainforest Biomass Based on Remote Sensing Data

Quantitative research on forest biomass in large-scale areas plays an important role in affirming the role of forest vegetation in the global carbon cycle and the role of forest ecosystems in the context of climate change. Traditional approaches based on field measurements are highly accurate but are only suitable for small research scopes and are difficult to carry out over large areas. With groundbreaking progress in the quantitative collection of forest parameters, such as forest height and canopy density, remote sensing has become the main source of data for biomass estimation [50,51]. Combining active and passive remote sensing in forest biomass estimates provides a useful solution for the estimation of carbon reserves and evaluation of forest ecosystems [52].

In this study, we compared methods for estimating the biomass of forest ecosystems in the Kon Ha Nung Plateau area based on four basic regression models. We identified the optimal models for 2016 (lin-log model with $R^2 = 0.72$) and 2021 (log-lin model, $R^2 = 0.73$), with results equivalent to those of a Landsat-8 image application in a Zagros oak forest study ($R^2 = 0.73$) [53] or that in Fonseca's study using Advanced Land-Observing Satellite (ALOS; $R^2 = 0.71$) [54]. Using basic regression models allows us to determine the correlation between remote sensing imagery and real biomass from forest investigation standard cells, enhancing the accuracy of the biomass estimation results that many studies have used [55,56]. In Norway, the abovementioned authors have also used a log model to estimate forest reserves, with an R^2 factor ranging between 0.83 and 0.97 [31], much higher

than our study. Similarly, the logarithmic model has also been applied in Ontario, with an R^2 factor of 0.82 to 0.90 (RMSE: 48.07–66.65) [32].

Sentinel-2 remote sensing imagery (10 m × 10 m) is a suitable tool for biomass research over large-scale areas, providing high accuracy [57]. In this study, Sentinel-2 imagery provided correlation coefficients for 2016 and 2021 of 0.72 and 0.73, respectively. These values were higher than those for the Landsat-8 satellite image data (30 m × 30 m), which only reached 0.5910 before correction and 0.6704 after correction [58]; the 2011 Landsat data applied to the National Nature Reserve of Yaoluoping in Anhui Province, where the R^2 was only 0.61 for coniferous forests and 0.63 for broadleaf forests [33]; or the use of Landsat photos for multitemporal evaluation from 1984 to 2016 in Canada, with R^2 reaching 0.70 [59]. In addition, to enhance the R^2 correlation coefficient value, it is possible to combine satellite imagery and SAR-based Advanced Land-Observing Satellite (ALOS) Phased Array type L-band Synthetic Aperture Radar (PALSAR) in forest biomass research [60] or data captured by UAVs [61].

In this study, the EVI for plants based on remote sensing imagery was applied to estimate forest vegetation biomass, similar to the methods of Brazil [62]. The NDVI and EVI are the most frequently used indicators for primary productivity and have been commonly used in vegetation studies [46,63,64].

4.2. Status Quo and Fluctuations of Biomass in the Kon Ha Nung Plateau Area for the Period 2016–2021

The results of the biomass estimates in the Kon Ha Nung Plateau area indicated that the biomass values of natural forest vegetation were quite high, reaching average values of 90 Mg/ha in 2016 and 105 Mg/ha in 2021. These are high values compared to the natural forest biomass value in Australia as determined using Landsat images (averages of 72.9 and 85.7 Mg/ha); in Gabon, the forest biomass value was only 63.3 Mg/ha, or in Madagascar, the average biomass value was 81 Mg/ha [65]. However, the biomass value in the Kon Ha Nung Plateau area is still quite low compared to other tropical rainforest areas in the world, such as in French Guiana which reached a value of 250–500 Mg/ha [66].

The results of our study demonstrated that, in the Kon Ha Nung Plateau area, biomass values as well as the ability to store carbon and absorb CO_2 of tropical rainforest vegetation showed positive changes, with the results indicating increases over the period 2016–2021. Forestry policies for forest ecosystems have a positive impact on increasing AGB, especially for nature reserves or national parks [56]. Forestry policies are paramount in forest management, as they guide the actions of foresters or natural resource managers at a given location [67]. In recent years, forestry policies on forest protection, protection of natural forest ecosystems, and biodiversity conservation in the Kon Ha Nung Plateau area have been significantly promoted, especially policies on forest protection and payment of forest environmental services. In Vietnam, payments for forest environmental services are gradually becoming popular with forest management communities; however, they have not become a stable source of income for local people, limiting the effectiveness of forest environmental services [68]. In the long run, the management and protection of forests and biodiversity must still be associated with the lives of indigenous peoples in forested areas. Appropriate policies of the state, the culture of indigenous peoples, an understanding of the nature, and skills to adapt to the environment related to forests contribute to socioeconomic development associated with the protection and development of forests, as well as biodiversity conservation (for the Kon Ha Nung Plateau area in particular and mountainous areas in general) [69].

Survey data and surveys of forest standard plots serve as the basis for estimating the biomass, as well as carbon sequestration capacity, of tropical rainforests. As forest survey standard cell data were inherited from the results of different projects, the locations of the 2016 and 2021 standard cells differed. In addition, the number of forest standard plots underlying the 2016 biomass estimate was not large—with only 19 cells—while we used 44 cells in 2021. To determine biomass fluctuations and carbon sequestration capacity of

tropical rainforests through several stages, there is a need for uniformity between surveys and field surveys in each stage. In this study, we only applied Sentinel-2 images at a single time of year as the best quality image acquisition time due to a lack of clouds. However, for enhanced accuracy, remote sensing images can be used at different times of the year to estimate the biomass of tropical rainforests. The drawback of optical remote sensing is that only the terrestrial biomass of plants can be identified. To determine subterranean biomass, separate measurements and calculation methods are needed.

5. Conclusions

Identifying the biomass of forest vegetation plays an important role in the global carbon cycle, as biomass serves as a source of carbon storage, absorbs CO_2, and contributes to adaptation to climate change. Remote sensing has become a powerful supporting tool for the estimation of forest ecosystem biomass at a large scale. Based on Sentinel-2 satellite imagery from 2016 and 2021 combined with data from standard forest survey cells, a model of natural forest vegetation biomass was established for the Kon Ha Nung Plateau area, Vietnam.

In this study, we developed a process for estimating biomass and carbon sequestration for tropical rainforest areas based on free medium-resolution satellite imagery. This can serve as a basis for managers to apply carbon tax programs in tropical rainforest areas, which are still lacking in developing countries, including Vietnam.

In the near future, with the development of satellite imagery, we may be able to estimate the biomass and carbon sequestration capacity of tropical rainforest ecosystems with greater accuracy. In addition, there is a need for field surveys that provide additional data on real biomass measurements, according to forest standard plots, to enhance the accuracy of biomass estimation models.

Author Contributions: The authors participated in the following specific aspects of article preparation: H.N.D. built the structure of the article, described the characteristics of the study area, and contributed to the discussion of the results; D.D.B. and D.N.T. conceived and designed the study; D.D.B. and D.N.T. wrote the draft; D.D.B., D.N.T. and H.N.H.V. analyzed the data; D.D.B. provided the remote sensing images; and D.D.B. wrote the final paper. All authors have read and agreed to the published version of the manuscript.

Funding: This research received no external funding.

Institutional Review Board Statement: Not applicable.

Informed Consent Statement: Not applicable.

Data Availability Statement: Data is contained within the article.

Acknowledgments: The authors would like to acknowledge the project "Research on biomass fluctuations and carbon exchange capacity in forest ecosystems in Kon Ha Nung Plateau, Gia Lai province" chaired by the Institute of Tropical Ecology, Joint Vietnam–Russia Tropical Science and Technology Research Center, which provided data and supported the field survey process of the authors. We would also like to sincerely thank the reviewers for their helpful comments, which helped us to improve this article.

Conflicts of Interest: The authors declare no conflict of interest.

References

1. Ollinger, S. *Forest Ecosystems. In Encyclopedia of Life Sciences*; Nature Publishing Group: London, UK, 2003.
2. Jim, C.Y. Effect of vegetation biomass structure on thermal performance of tropical green roof. *Landsc. Ecol. Eng.* **2012**, *8*, 173–187. [CrossRef]
3. Corlett, R.; Primack, R. *Tropical Rain Forests: An Ecological and Biogeographical Comparison*, 2nd ed.; John Wiley and Sons: Hoboken, NJ, USA, 2011.
4. Brown, S.; Gillespie, A.; Lugo, A. Biomass Estimation Methods for Tropical Forests with Applications to Forest Inventory Data. *For. Sci.* **1989**, *35*, 881–902.

5. Brown, S. *Estimating Biomass and Biomass Change of Tropical Forests: A Primer*; FAO Forester Paper; FAO: Rome, Italy, 1997; Volume 134.
6. Brown, S. Measuring carbon in forests: Current status and future challenges. *Environ. Pollut.* **2002**, *116*, 363–372. [CrossRef] [PubMed]
7. Macdicken, K. *A Guide to Monitoring Carbon Storage in Forestry and Agroforestry Projects*; Winrock International Institute for Agricultural Development: Little Rock, AR, USA, 1997.
8. Ketterings, Q.; Coe, R.; Van Noordwijk, M.; Ambagau', Y.; Palm, C. Reducing uncertainty in the use of allometric biomass equations for predicting above-ground tree biomass in mixed secondary forest. *For. Ecol. Manag.* **2001**, *146*, 199–209. [CrossRef]
9. Houghton, R. Aboveground Forest Biomass and the Global Carbon Balance. *Glob. Chang. Biol.* **2005**, *11*, 945–958. [CrossRef]
10. Henry, M.; Besnard, A.; Asante, W.; Eshun, J.; Adu-Bredu, S.; Valentini, R.; Bernoux, M.; Saint-Andre, L. Wood density, phytomass variations within and among trees, and allometric equations in a tropical rainforest of Africa. *For. Ecol. Manag.* **2010**, *260*, 1375–1388. [CrossRef]
11. Henry, M.; Cifuentes, M.; Réjou-Méchain, M.; Piotto, D.; Michel, J.M.; Wayson, C.; Alice Guier, F.; Lombis, H.; Castellanos, E.; Lara, R.; et al. Recommendations for the use of tree models to estimate national forest biomass and assess their uncertainty. *Ann. For. Sci.* **2015**, *72*, 769–777. [CrossRef]
12. Raj, A.; Jhariya, M.K. Site quality and vegetation biomass in the tropical Sal mixed deciduous forest of Central India. *Landsc. Ecol. Eng.* **2021**, *17*, 387–399. [CrossRef]
13. Chave, J.; Andalo, C.; Brown, S.; Cairns, M.; Chambers, J.; Eamus, D.; Fölster, H.; Fromard, F.; Higuchi, N.; Kira, T.; et al. Tre allometry and improved estimation of carbon stocks and balance in tropical forests. *Oecologia* **2005**, *145*, 87–99. [CrossRef] [PubMed]
14. Chave, J.; Réjou-Méchain, M.; Burquez, A.; Chidumayo, E.; Colgan, M.; Delitti, W.; Duque, A.; Eid, T.; Fearnside, P.; Goodman, R.; et al. Improved allometric models to estimate the aboveground biomass of tropical trees. *Glob. Change Biol.* **2014**, *20*, 3177–3190. [CrossRef] [PubMed]
15. Temesgen, H.; Goerndt, M.; Johnson, G.; Adams, D.; Monserud, R. Forest Measurement and Biometrics in Forest Management: Status and Future Needs of the Pacific Northwest USA. *J. For.* **2007**, *105*, 233–238.
16. Temesgen, H.; Affleck, D.; Poudel, K.; Gray, A.; Sessions, J. A Review of the Challenges and Opportunities in Estimating Above Ground Forest Biomass Using Tree-Level Models. *Scand. J. For. Res.* **2015**, *30*, 326–335. [CrossRef]
17. Zhang, L. Cross-Validation of Non-Linear Growth Functions for Modeling Tree Height-Diameter Relationships. *Ann. Bot.* **1997**, *79*, 251–257. [CrossRef]
18. Picard, R.; Cook, R. Cross-Validation of Regression Models. *J. Am. Stat. Assoc.* **1984**, *79*, 575–583. [CrossRef]
19. Lu, D. Aboveground biomass estimation using Landsat TM data in the Brazilian Amazon. *Int. J. Remote Sens.* **2005**, *26*, 2509–2525. [CrossRef]
20. Nelson, R.; Kimes, D.; Salas, W.; Routhier, M. Secondary Forest Age and Tropical Forest Biomass Estimation Using Thematic Mapper Imagery. *BioScience* **2009**, *50*, 419–431. [CrossRef]
21. Steininger, M. Satellite estimation of tropical secondary forest above-ground biomass: Data from Brazil and Bolivia. *Int. J. Remote Sens.* **2000**, *21*, 1139–1157. [CrossRef]
22. Zheng, D.; Rademacher, J.; Chen, J.; Crow, T.; Bresee, M.; Moine, J.; Ryu, S. Estimating aboveground biomass using Landsat 7 ETM+ data across a managed landscape in northern Wisconsin, USA. *Remote Sens. Environ.* **2004**, *93*, 402–411. [CrossRef]
23. Rosillo-Calle, F.; Woods, J. *The Biomass Assessment Handbook*; Routledge: London, UK, 2012.
24. Natarajan, K.; Latva-Käyrä, P.; Zyadin, A.; Pelkonen, P. New methodological approach for biomass resource assessment in India using GIS application and land use/land cover (LULC) maps. *Renew. Sustain. Energy Rev.* **2016**, *63*, 256–268. [CrossRef]
25. Zyadin, A.; Natarajan, K.; Latva-Käyrä, P.; Igliński, B.; Iglińska, A.; Trishkin, M.; Pelkonen, P.; Pappinen, A. Estimation of surplus biomass potential in southern and central Poland using GIS applications. *Renew. Sustain. Energy Rev.* **2018**, *89*, 204–215. [CrossRef]
26. Nguyen, L.D.; Nguyen, C.T.; Le, H.S.; Tran, B.Q. Mangrove Mapping and Above-Ground Biomass Change Detection using Satellite Images in Coastal Areas of Thai Binh Province, Vietnam. *For. Soc.* **2019**, *3*, 248–261. [CrossRef]
27. Li, T.; Mausel, P.; Brondízio, E.; Deardorff, D. A framework for creating and validating a non-linear spectrum-biomass model to estimate the secondary succession biomass in moist tropical forests. *ISPRS J. Photogramm. Remote Sens.* **2010**, *65*, 241–254. [CrossRef]
28. Lu, D.; Mausel, P.; Brondízio, E.; Moran, E. Relationships between forest stand parameters and Landsat TM spectral responses in the Brazilian Amazon Basin. *For. Ecol. Manag.* **2004**, *198*, 149–167. [CrossRef]
29. Lu, D.; Chen, Q.; Wang, G.; Moran, E.; Batistella, M.; Zhang, M.; Vaglio Laurin, G.; Saah, D. Aboveground Forest Biomass Estimation with Landsat and LiDAR Data and Uncertainty Analysis of the Estimates. *Int. J. For. Res.* **2012**, *2012*, 436537. [CrossRef]
30. Kronseder, K.; Ballhorn, U.; Boehm, H.-D.; Siegert, F. Above ground biomass estimation across forest types at different degradation levels in Central Kalimantan using LiDAR data. *Int. J. Appl. Earth Obs. Geoinf.* **2012**, *18*, 37–48. [CrossRef]
31. Næsset, E. Effects of different flying altitudes on biophysical stand properties estimated from canopy height and density measured with a small foot-print airborne scanner. *Remote Sens. Environ.* **2004**, *91*, 243–255. [CrossRef]
32. Lim, K.; Treitz, P. Estimation of above ground forest biomass from airborne discrete return laser scanner data using canopy-based quantile estimators. *Scand. J. For. Res.* **2004**, *19*, 558–570. [CrossRef]

33. Yang, B.; Zhang, Y.; Mao, X.; Lv, Y.; Shi, F.; Li, M. Mapping Spatiotemporal Changes in Forest Type and Aboveground Biomass from Landsat Long-Term Time-Series Analysis—A Case Study from Yaoluoping National Nature Reserve, Anhui Province of Eastern China. *Remote Sens.* **2022**, *14*, 2786. [CrossRef]
34. Wang, L.; Sousa, W. Distinguishing mangrove species with laboratory measurements of hyperspectral leaf reflectance. *Int. J. Remote Sens.* **2009**, *30*, 1267–1281. [CrossRef]
35. Sharma, S.B.; Kumar, S.; Hegde, N. Biomass and carbon recovery of secondary forest in a Montane Subtropical Forest of North Eastern India. *Trop. Ecol.* **2022**, 1–8. [CrossRef]
36. Do, T.V.; Yamamoto, M.; Kozan, O.; Hai, V.; Phung, D.; Thang, N.; Hai, L.; Nam, V.; Trieu, H.; Hoang, T.; et al. Ecoregional variations of aboveground biomass and stand structure in evergreen broadleaved forests. *J. For. Res.* **2019**, *31*, 1713–1722. [CrossRef]
37. Gibbs, H.; Brown, S.; Niles, J.; Foley, J. Monitoring and estimating tropical forest carbon stocks: Making REDD a reality. *Environ. Res. Lett.* **2007**, *2*, 045023. [CrossRef]
38. Pandian, E.; Parthasarathy, N. Decadal (2003–2013) changes in liana diversity, abundance and aboveground biomass in four inland tropical dry evergreen forest sites of peninsular India. *J. For. Res.* **2015**, *27*, 133–146. [CrossRef]
39. Wanyonyi, P.; Tsingalia, M.; Omayio, D.; Mzungu, E. Evidence of Climate Changes in a Tropical Rainforest: Case Study Kakamega Tropical Rainforest. *Int. J. Environ. Clim. Change* **2021**, *11*, 202–2012. [CrossRef]
40. Mauya, E.; Madundo, S. Aboveground biomass and carbon stock of usambara tropical rainforests in Tanzania. *Tanzan. J. For. Nat. Conserv.* **2021**, *90*, 63–82.
41. Foody, G.; Curran, P. Estimation of Tropical Forest Extent and Regenerative Stage Using Remotely Sensed Data. *J. Biogeogr.* **1994**, *21*, 223. [CrossRef]
42. Institute of Ecology and Biological Resources. *Building a Profile of the World Biosphere Reserve on the Kon Ha Nung Plateau*; People's Committee of Gia Lai Province: Pleiku, Vietnam, 2020.
43. Quynh, H. Geographical basic for management and sustainable using and environment protection of Kon Ka Kinh national park, Gia Lai province. *Vietnam J. Earth Sci.* **2014**, *36*, 175–183. [CrossRef]
44. Do, H.; Grant, J.; Bon, T.; Zimmer, H.; Nichols, J. Diversity depends on scale in the forests of the Central Highlands of Vietnam. *J. Asia-Pac. Biodivers.* **2017**, *10*, 472–488. [CrossRef]
45. Nguyen Dang, H. *Features of Anthroprogenic Landscape Kon Ka Kinh National Park and Its Vicinity*; Vietnam—Russian Tropical Center: Hanoi, Vietnam, 2017.
46. Jinru, X.; Su, B. Significant Remote Sensing Vegetation Indices: A Review of Developments and Applications. *J. Sens.* **2017**, *2017*, 1353691. [CrossRef]
47. Liu, H.Q.; Huete, A.R. A feedback based modification of the NDVI to minimize canopy background and atmospheric noise. *IEEE Trans. Geosci. Remote Sens.* **1995**, *33*, 457–465. [CrossRef]
48. Gujarati, D. *Econometrics by Example*; Bloomsbury Publishing: London, UK, 2014.
49. Applied Statistics. Lesson 5: Correlation Coefficients. Available online: http://www.andrews.edu/~{}calkins/math/edrm611/edrm05.htm (accessed on 18 July 2005).
50. Li, D.; Wang, C.; Hu, Y.; Liu, S. General review on remote sensing-based biomass estimation. *Geomat. Inf. Sci. Wuhan Univ.* **2012**, *37*, 631–635.
51. Wei, X. Biomass Estimation: A Remote Sensing Approach. *Geogr. Compass* **2010**, *4*, 1635–1647. [CrossRef]
52. Gao, L.; Chai, G.; Zhang, X. Above-Ground Biomass Estimation of Plantation with Different Tree Species Using Airborne LiDAR and Hyperspectral Data. *Remote Sens.* **2022**, *14*, 2568. [CrossRef]
53. Safari, A.; Sohrabi, H.; Powell, S. Comparison of satellite-based estimates of aboveground biomass in coppice oak forests using parametric, semiparametric, and nonparametric modeling methods. *J. Appl. Remote Sens.* **2018**, *12*, 046026. [CrossRef]
54. Fonseca, G.; Soares, V.; Leite, H.; Ferraz, A.; Ribeiro, C.; Lorenzon, A.; Marcatti, G.; Teixeira, T.; Castro, N.; Mota, P.; et al. Artificial neural networks on integrated multispectral and SAR data for high-performance prediction of eucalyptus biomass. *Comput. Electron. Agric.* **2020**, *168*, 105089. [CrossRef]
55. Galeana-Pizaña, J.; Núñez, J.M.; Corona, N. Remote Sensing-Based Biomass Estimation. In *Evironmental Applications of Remote Sensing*; IntechOpen: London, UK, 2016.
56. Wu, C.; Shen, H.; Wang, K.; Shen, A.; Deng, J.; Gan, M. Landsat Imagery-Based Above Ground Biomass Estimation and Change Investigation Related to Human Activities. *Sustainability* **2016**, *8*, 159. [CrossRef]
57. Vinué-Visús, D.; Ruiz-Peinado, R.; Fuente, D.; Oliver-Villanueva, J.-V.; Coll-Aliaga, E.; Lerma-Arce, V. Biomass Assessment and Carbon Sequestration in Post-Fire Shrublands by Means of Sentinel-2 and Gaussian Processes. *Forests* **2022**, *13*, 771. [CrossRef]
58. Yu, Y.; Pan, Y.; Yang, X.; Fan, W. Spatial Scale Effect and Correction of Forest Aboveground Biomass Estimation Using Remote Sensing. *Remote Sens.* **2022**, *14*, 2828. [CrossRef]
59. Matasci, G.; Hermosilla, T.; Wulder, M.; White, J.; Coops, N.; Hobart, G.; Bolton, D.; Tompalski, P.; Bater, C. Three decades of forest structural dynamics over Canada's forested ecosystems using Landsat time-series and lidar plots. *Remote Sens. Environ.* **2018**, *216*, 697–714. [CrossRef]
60. Wang, X.; Liu, C.; Lv, G.; Xu, J.; Cui, G. Integrating Multi-Source Remote Sensing to Assess Forest Aboveground Biomass in the Khingan Mountains of North-Eastern China Using Machine-Learning Algorithms. *Remote Sens.* **2022**, *14*, 1039. [CrossRef]

61. Wang, F.; Yang, M.; Ma, L.; Zhang, T.; Qin, W.; Li, W.; Zhang, Y.; Sun, Z.; Wang, Z.; Li, F.; et al. Estimation of Above-Ground Biomass of Winter Wheat Based on Consumer-Grade Multi-Spectral UAV. *Remote Sens.* **2022**, *14*, 1251. [CrossRef]
62. Freitas Silva, Y.; Valadares, R.; Werner, J.; Figueiredo, G.; Campbell, E. Spatial analysis of aboveground biomass and the enhanced vegetation index. In Proceedings of the AGU Fall Meeting, San Francisco, CA, USA, 9–13 December 2019.
63. Garroutte, E.; Hansen, A.; Lawrence, R. Using NDVI and EVI to Map Spatiotemporal Variation in the Biomass and Quality of Forage for Migratory Elk in the Greater Yellowstone Ecosystem. *Remote Sens.* **2016**, *8*, 404. [CrossRef]
64. Munyati, C. Detecting the distribution of grass aboveground biomass on a savannah rangeland using Sentinel-2 MSI vegetation indices. *Adv. Space Res.* **2021**, *69*, 1130–1145. [CrossRef]
65. El Hajj, M.; Baghdadi, N.; Fayad, I.; Vieilledent, G.; Bailly, J.-S.; Ho Tong Minh, D. Interest of Integrating Spaceborne LiDAR Data to Improve the Estimation of Biomass in High Biomass Forested Areas. *Remote Sens.* **2017**, *9*, 213. [CrossRef]
66. Liao, Z.; He, B.; Quan, X.; van Dijk, A.; Qiu, S.; Yin, C. Biomass estimation in dense tropical forest using multiple information from single-baseline P-band PolInSAR data. *Remote Sens. Environ.* **2019**, *221*, 489–507. [CrossRef]
67. Grebner, D.; Bettinger, P.; Siry, J.; Boston, K. Forest policies and external pressures. In *Introduction to Forestry and Natural Resources*; Academic Press: Cambridge, MA, USA, 2022; pp. 365–386.
68. Thuy, P.T.; Chau, N.H.; Chi, D.T.L.; Long, H.T.; Fisher, M.R. The politics of numbers and additionality governing the national Payment for Forest Environmental Services scheme in Vietnam: A case study from Son La province. *For. Soc.* **2020**, *4*, 379–404. [CrossRef]
69. Ngo, T.T.H.; Nguyen, T.P.M.; Duong, T.H.; Ly, T.H. Forest—Related Culture and Contribution to Sustainable Development in the Northern Mountain Region in Vietnam. *For. Soc.* **2021**, *5*, 32–47. [CrossRef]